Representing Functional Connectivity with Structural Detour: A New Perspective to Decipher Structure-Function Coupling Mechanism

Ziquan Wei[1,2][0000−0001−6553−4482], Tingting Dan[2], Jiaqi Ding[1,2], Paul Laurienti[3], and Guorong Wu[1,2](✉)

[1] Department of Computer Science, University of North Carolina at Chapel Hill, Chapel Hill, NC 27514, USA
ziquanw@email.unc.edu, jiaqid@cs.unc.edu

[2] Department of Psychiatry, University of North Carolina at Chapel Hill, Chapel Hill, NC 27514, USA
{Tingting_Dan, grwu}@med.unc.edu

[3] Department of Radiology, Wake Forest University School of Medicine, Winston-Salem, NC 27101, USA
plaurien@wakehealth.edu

Abstract. Modern neuroimaging technologies set the stage for studying structural connectivity (SC) and functional connectivity (FC) *in-vivo*. Due to distinct biological wiring underpinnings in SC and FC, however, it is challenging to understand their coupling mechanism using statistical association approaches. We seek to answer this challenging neuroscience question through the lens of a novel perspective rooted in network topology. Specifically, our assumption is that each FC instance is either locally supported by the direct link of SC or collaboratively sustained by a group of alternative SC pathways which form a topological notion of *detour*. In this regard, we propose a new connectomic representation, coined detour connectivity (DC), to characterize the complex relationship between SC and FC by presenting direct FC with the weighted connectivity strength along in-directed SC routes. Furthermore, we present SC-FC Detour Network (SFDN), a graph neural network that integrates DC embedding through a self-attention mechanism, to optimize detour to the extent that the coupling of SC and FC is closely aligned with the evolution of cognitive states. We have applied the concept of DC in network community detection while the clinical value of our SFDN is evaluated in cognitive task recognition and early diagnosis of Alzheimer's disease. After benchmarking on three public datasets under various brain parcellations, our detour-based computational approach shows significant improvement over current state-of-the-art counterpart methods.

Keywords: Structure-function coupling · Structural connectivity · Functional connectivity · Network detour · Graph neural networks

1 Introduction

Since the precise influence of underlying structural connectivity (SC) on functional neural activity is pivotal in neuroscience, it is a major goal in the field to understand structure-function coupling and relationships [23, 24, 2, 30]. The techniques of diffusion-weighted imaging (DWI) and functional magnetic resonance imaging (fMRI) on whole-brain make it possible to measure system-level quantitative connectivity on structural and functional, respectively, revealing white-matter (WM) pathways and functional correlation. Thus, lifting the curtain on structure-function coupling is a vital step to discovering the enigma of the human brain using multi-modal data.

Structure-function coupling approaches are various from using biophysical models [14, 27], graph harmonics [24, 17], network communications [10], multivariate statistical technique [20], to deep learning-based structure-function mapping [5, 25, 22]. However, the correspondence between structural and functional connectivity is far from perfect [7] due to the unexpected absence of a direct structural link between regions that are functionally connected [13], especially on macroscale, such as the default mode network [21, 3]. The observation [10] of detour connections amplifying functional connectivity shows an opportunity for structural detours fetching up the absent direct structural connection. Consequently, the imperfect correspondence between structure and function could be caused by neglecting indirect anatomic pathways in functional connectivity (FC). This motivates us to propose the **detour connectivity** (DC).

Importantly, 'indirect' functional connections by structural detours support the emergence of canonical features of FC and geometry of the human brain [18]. Detour is meanwhile a metric in graph theory [6], and is also indispensable information in real-world networks. Such as detour route analysis in traffic tasks [9], tourism detour spots [12], and third-person (referring to a detour connection) effects on social-media [1] are real-world instances of network detour patterns contributing to practical applications.

The potential of DC is shown in Fig. 1. In the left, functional correlation shows denser edges than structural since most pairwise functional connections are not supported by a direct WM pathway [18]. The problem of such significant gap is rooted in the limitation of current low-order network models which only characterize node-to-node relationships. Recurrent connection strength, on the other hand, is strongly associated with the specialization of behavior in group test [27], since cognitive behavior is derived by network communities shaped as cycles. To address this challenge, we put the spotlight on the (high-level) structural detour paired with each FC. As shown in the right panel of Fig. 1, we measure detouring links fetching up individual differences by considering 'indirect' links so that the connectivity represents brain network communities.

Furthermore, we design a Transformer-style GNN framework named **SC-FC Detour Network** (SFDN) to efficiently combine SC and FC for GNN on multimodal MRI data. SFDN benefits from the architecture of the self-attention mechanism, such that feature representation can involve edge-wise DC embed-

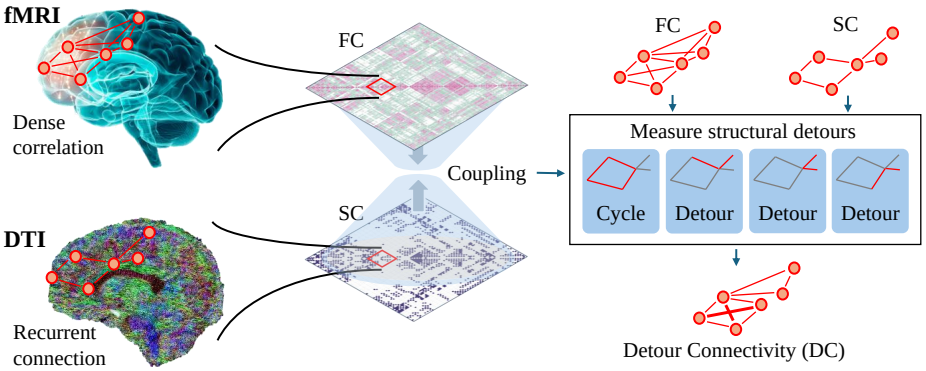

Fig. 1. Left: Structure-function coupling remains challenging since FC from fMRI is dense and recurrent connection in SC by DTI is strongly associated with the individual. Right: Detour connectivity (DC, See Def. 2) measures cyclic and detouring links of individual SC to weight FC. Detouring links are simultaneously present in cyclic structure and incomplete cycles addressing various SC of individuals.

ding for high-order interactions between brain regions among macroscale networks. Hence, yielding accurate predictions on human cognition.

In experiments, we evaluate the proposed methods on three public datasets, HCP-A, ADNI, and OASIS (see Sec. 3), by group-wise t-tests, cognitive state detection, and disease classification. Two different atlas, two baselines, and different lengths of fMRI are used for robustness. We find that DC performs effectively in network community detection, suggesting a trustful structure-function coupling, and a remarkable improvement of accuracy is demonstrated by SFDN on both three datasets, after a comprehensive evaluation with respect to various brain atlases, current state-of-the-arts, and multi-site fMRI data. Codes of our experiments are released[1].

2 Methods

Notations. Assume SC and FC are denoted by adjacency matrices $\mathbf{A}^S \in \mathbb{R}^{N\times N}$ and $\mathbf{A}^F \in \mathbb{R}^{N\times N}$, respectively, where $A^{\cdot}_{ij}$ is the connectivity between i^{th} and j^{th} region. In practice, SC and FC are calculated by the subject-wise normalized WM pathway counting and the correlation coefficient of neural signals, respectively. $\hat{\mathbf{A}}^{\cdot}$ is the binary adjacency matrix after high-pass filtering and self-loop removal. In this work, high-pass filters are different thresholds of WM pathway counting and functional correlation. $|\cdot|$ means the cardinality of a set.

2.1 Detour Connectivity

Definition 1 (structural detour (SD)). *SD is a pathway in the topology of SC between functionally connected regions. It is defined as indirect path and is*

[1] https://github.com/Chrisa142857/SC-FC-Detour

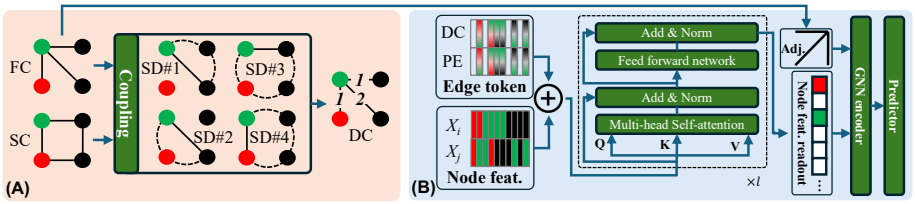

Fig. 2. (A) Detour connectivity (DC) obtained by structure-function coupling. (B) The flowchart of SFDN. It takes DC and FC topology as input, where PE stands for positional encoding, 'Adj.' stands for adjacency matrix, and 'feat.' stands for features.

obtained by a Depth-First Search, $DFS(\hat{\mathbf{A}}^S, i, j, k)$ *if* $\hat{A}^F_{ij} > 0$*, where* k *is the maximum searching radius. The searching result is the set of SD, each element (path) is a node set and includes only the indirect path that has 3 or more nodes.*

Definition 2 (detour connectivity (DC)). *DC is denoted by* $\mathbf{A}^D \in \mathbb{R}^{N\times N}$*, where* $A^D_{ij} = |DFS(\hat{\mathbf{A}}^S, i, j, k)|$ *if* $\hat{A}^F_{ij} > 0$*, otherwise being zero.*

For example, given a subject with SC and FC, as shown in Fig. 2 (A), the proposed DC measures the number of SDs denoted by dashed curves corresponding to edges of FC that are denoted by solid lines. After structure-function coupling, the edges of the FC graph are weighted and followed by training an end-to-end graph transformer with the edge-wise embedding DC.

2.2 SC-FC Detour Network (SFDN)

Applying the edge-wise DC to GNN, we design SFDN as shown in Fig. 2 (B). DC weights and FC positional encoding (PE) are first embedded as edge-wise tokens, where PE is defined, e.g., for an edge $\overrightarrow{ij}$, by the concatenation of i^{th} and j^{th} eigenvectors of graph Laplacian matrix $\mathbf{L} := diag(\left[\sum_{b=1}^{N} \hat{A}^F_{ab}\right]_{a=1,\cdots,N}) - \hat{\mathbf{A}}^F$, and hence it can be node permutation invariant. As illustrated by color bars on the left top in (B), an edge token is formed by concatenating DC and PE and empty bars indicate zeros to hold the token place for node feature readout at the end. On the left bottom in (B), the node features X_i and X_j corresponding to edge tokens for an edge $\overrightarrow{ij}$ are also concatenated to add with the edge token after a learnable mapping. Note that the node feature is filled by stacking the same initial node feature twice for an empty edge token so that the readout has enough information.

Afterward, tokens are element-wise added ($\bigoplus$) with node features and passed to l self-attention blocks in the middle in (B). Each block firstly maps tokens to queries ($\mathbf{Q}$), keys ($\mathbf{K}$), and values ($\mathbf{V}$) and is followed by multi-head self-attention $softmax(\frac{\mathbf{Q}\mathbf{K}^T}{\sqrt{d}})\mathbf{V}$ with a feed-forward network and a multi-layer perceptron (MLP). To the end, GNN takes $\hat{\mathbf{A}}^F$ and the node readout as input to encode the graph, then a predictor produces the final graph-level prediction.

3 Experimental results

Preprocessing and datasets. To thoroughly evaluate our methods, three public datasets are used in our experiments. Three public tools, CONTINUITY, fmriprep, and smriprep, are used for the data to acquire SC and FC with an arbitrary atlas. Default hyperparameters[2] are set during our experiments.

The Lifespan Human Connectome Project Aging (HCP-A) dataset [4] is instrumental in task recognition research, offering a comprehensive view of the aging process. It includes data from 717 subjects, encompassing both fMRI (n=4,846) and DWI (n=717). It includes data from four brain tasks associated with memory: VISMOTOR, CARIT, FACENAME, and resting state. In the related experiments, these tasks are treated as (1) four groups for group analysis and (2) a four-class classification problem. The details of data preprocessing can be found in supplementary. We partition brain regions using Gordon [11] or AAL [26], to obtain SC and FC.

Alzheimer's Disease Neuroimaging Initiative (ADNI) dataset [28] serves as an invaluable resource, featuring a collection of fMRI (n=250) and preprocessed SC (n=1,012) with AAL parcellation. In our experiment, 135 subjects among the dataset that have undergone both DWI and fMRI scans are included so that structure-function coupling is feasible. Additionally, ADNI includes clinical diagnostic labels, encompassing a spectrum of cognitive states: Cognitive Normal (CN), Subjective Memory Complaints (SMC), Early-Stage Mild Cognitive Impairment (EMCI), Late-Stage Mild Cognitive Impairment (LMCI), and Alzheimer's Disease (AD). Considering the data balance issue, we simplified these categories into two broad groups based on disease severity: we combined CN, SMC, and EMCI into 'CN' group, while LMCI and AD were grouped as the 'AD' group.

Open Access Series of Imaging Studies (OASIS) dataset [16] presents a substantial collection of data from 924 subjects, comprising 3,322 fMRI sessions in total. Each subject has fMRI and DWI and is processed with Destrieux parcellation [8]. Our experiment focused on binary classification: subjects in preclinical stages of AD or those manifesting dementia-related conditions are under the 'AD' group, while healthy individuals are under the 'CN' group.

Experimental settings. Our experiments consist of (1) a paired t-test for group analysis on the HCP-A dataset and (2) accuracy comparisons between baselines and the proposed SFDN on three datasets. Thresholds of high-pass filtering are set as 0.1 and 0.5 for SC and FC, respectively, and $k = 5$ for measuring DC.

1) Group analysis. The proposed measurement of SC-FC coupling is expected to group-wise express brain network communities that are functionally related to a cognitive state. In this regard, group analysis is set as a paired t-test for the sum of each parcel DC per subject between four groups. In comparison, the sum of FC is tested in the same way for each parcel to show the effectiveness of detour connectivity. Among t-test results, significant parcels are obtained by filtering the p-value smaller than 0.05. Gordon parcellation has a fine partition

[2] https://github.com/NIRALUser/CONTINUITY, https://www.nipreps.org

($N = 330$) of the brain and is used in this experiment to show if the results of constructing communities functionally matched with the community defined by the atlas. Better and trustful performance of the proposed measurement is hence demonstrated by the distribution of significant parcel numbers focusing on network communities that have functions for the cognitive task.

2) Accuracy comparison. To show how accurate the proposed SFDN that is driven by DC, we choose graph convolution network (GCN) [15] and graph isomorphism network (GIN) [29] as baselines with the same hyperparameter settings on training and testing, each of which has 4 hidden layers with 768 channels. Node feature is initialized by SC. Layer number $l = 2$ with 2 heads for each layer of SFDN. Experiments run on both three datasets with statistic FC by using correlation of full-length fMRI, as well as dynamic FC is calculated on the HCP-A dataset to validate DC is effective with 100-length time courses by sliding window. Each result is the average of 5-fold cross-validation with 30-epoch training per fold and is compared by accuracy and weighted F1-score.

3.1 Group analysis of DC

The proposed structure-function coupling measurement DC is expected to be significant in corresponding macroscale brain networks of subjects in a specific cognitive task. Thus, we run a group analysis of DC for the task state against the resting state of each subject to show if functionally related brain networks have a significant difference by paired t-test, such as Visual network (VN) and SensoriMotor (SM) network for the VISMOTOR cognitive task (Fig. 3, right).

As shown in Fig. 3, the distribution of percentages parcels among a brain community that is significantly different with resting state is various between Gordon communities by DC. In contrast, FC shows slight differences between communities, even though the most of regions are significant on three cognitive task states. For instance, two SM networks, the dorsal attention network (DAN), default mode network (DMN), and VN are consistently high by DC. These three communities are active when clicking buttons and staring at the screen during VISMOTOR [4], and DMN is active during the resting state [19]. Such results of DC reflect functional activities on corresponding macroscale networks. While FC shows all communities are significant on all tasks caused by the individual specialization before structure-function coupling. For descriptions of community abbreviation in x-axis, see supplementary.

In addition, as shown in Fig. 4, the visualization of p-value of parcels on the WM surface clearly illustrates communities for the VISMOTOR group being differentiated from the resting state. The observation on detour connectivity supports the distribution in Fig. 3 that DC expressed high-order information between parcels among functionally matched macroscale networks, which are circled by dashed lines. VISMOTOR task in Fig. 4 requires participants to view checkerboards on the screen and make motor responses (button presses) indicating which side of the checkerboard shows a color change. As it is designed to engage visual and motor networks, VN and SM networks respectively circled by white and green show lower p-values compared to other networks. Apart

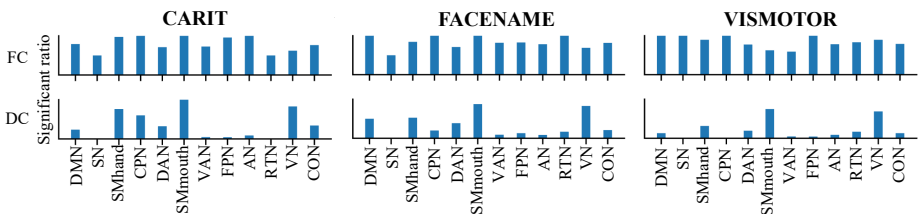

Fig. 3. The ratio distribution of parcels among the corresponding community of Gordon atlas [11] that are significantly different ($p \leq 0.05$) with resting state. Higher ratio means more significant parcels appeared in a macroscale network. It is evident that our DC measurements show a more pronounced task-to-task difference than conventional FC measurements, indicating a greater group-wise separation across tasking-states.

from that DC reflects the high significance of macroscale networks, it also implies that DC is a trustful measurement since highlighted communities other than VN, SM, and DMN are small and less significant (higher p-value), such as Cingulo-Opercular Network in cyan and Dorsal Attention Network in yellow.

In contrast, FC highlights parcels are more than DC and are mostly all significant, which hardly provides a clue of geometry information for recognizing functional activities by which macroscale networks. This agrees with the relatively flat distribution shown in Fig. 3 without measuring structural detours. SC is unchanged in Fig. 4 comparing different cognitive states by the same subject. Apparently, the group comparison results by our DC measurement not only closely align with current neuroscience research [4] but also manifest significant improvement over conventional method.

Table 1. Accuracy comparison between SFDN with baselines on HCP-A, where 'Stat.' stands for statistic, 'Dyn.' for dynamic, 'Avg. Imp.' for average improvement by SFDN, and 'Acc.' for accuracy.

		GCN		GIN		SFDN (GCN)		SFDN (GIN)		Avg. Imp.
		AAL	Gordon	AAL	Gordon	AAL	Gordon	AAL	Gordon	
Stat.	Acc.	$85.96_{\pm 1.2}$	$91.38_{\pm 1.0}$	$88.28_{\pm 0.8}$	$92.39_{\pm 2.4}$	$90.51_{\pm 0.7}$	$\mathbf{93.22}_{\pm 1.2}$	$89.85_{\pm 0.5}$	$91.99_{\pm 1.8}$	1.89
	F1	$85.81_{\pm 1.1}$	$91.24_{\pm 1.1}$	$88.18_{\pm 0.7}$	$92.51_{\pm 2.3}$	$90.43_{\pm 0.6}$	$\mathbf{93.27}_{\pm 1.3}$	$89.87_{\pm 0.5}$	$92.06_{\pm 1.8}$	1.97
Dyn.	Acc.	$82.72_{\pm 0.9}$	$87.43_{\pm 1.3}$	$84.69_{\pm 1.2}$	$89.09_{\pm 1.4}$	$87.82_{\pm 1.3}$	$\mathbf{93.00}_{\pm 0.8}$	$85.58_{\pm 0.7}$	$90.10_{\pm 1.2}$	3.14
	F1	$82.35_{\pm 0.9}$	$87.35_{\pm 1.3}$	$84.44_{\pm 1.1}$	$89.10_{\pm 1.4}$	$87.66_{\pm 1.3}$	$\mathbf{93.04}_{\pm 0.7}$	$85.46_{\pm 1.0}$	$90.11_{\pm 1.1}$	3.26

3.2 Accuracy of cognitive state classification

Experiments of the four-class classification on the HCP-A dataset show the performance of SFDN is enhanced by DC embedding compared to two baselines using different atlas or lengths of fMRI time series. Results are listed in Table 1.

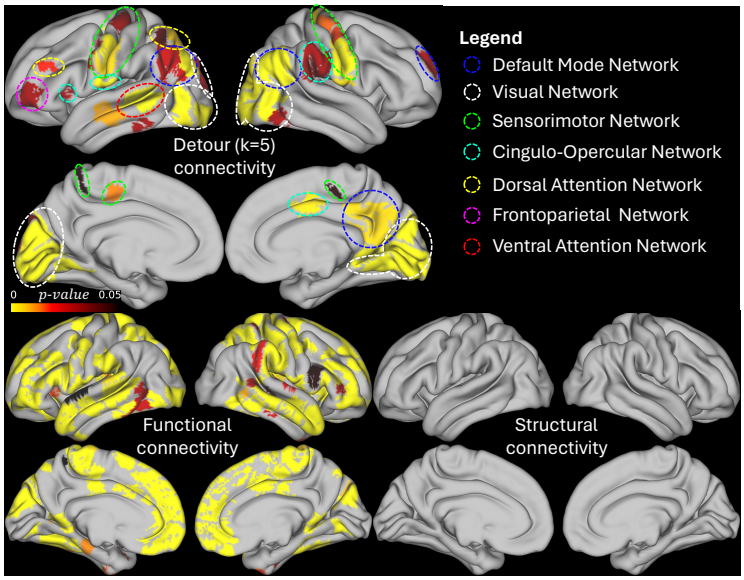

Fig. 4. The visualization of significant parcels by t-tests of DC, FC, and SC between the resting-state and VISMOTOR state, where p-value is produced by paired t-test.

The average improvement shown in the last column provides a quick overview of the effectiveness of SFDN in both static and dynamic FC. By increasing the accuracy and F1 score by approximately 2 and 3 points, respectively, SFDN demonstrates its efficacy. Altering baseline or atlas is common in brain cognition modeling research. DC is effective in all cases except for one, e.g., GCN accuracy using AAL on statistic FC is increased by 4.55 points using DC embedding.

Table 2. Accuracy comparison between SFDN with baselines on ADNI and OASIS datasets. Bold denotes the best of a dataset.

	GCN		GIN		SFDN (GCN)		SFDN (GIN)		Avg. Imp.
	ADNI	OASIS	ADNI	OASIS	ADNI	OASIS	ADNI	OASIS	
Acc.	$54.07_{\pm 34.4}$	$87.86_{\pm 3.4}$	$65.19_{\pm 16.1}$	**89.51**$_{\pm 2.5}$	**74.07**$_{\pm 17.2}$	$87.86_{\pm 3.2}$	$69.63_{\pm 14.7}$	$89.24_{\pm 2.9}$	6.04
F1	$45.39_{\pm 37.7}$	$82.21_{\pm 4.8}$	$65.73_{\pm 13.9}$	$86.46_{\pm 3.6}$	**70.20**$_{\pm 13.6}$	$83.76_{\pm 4.4}$	$70.14_{\pm 11.7}$	**86.82**$_{\pm 3.1}$	7.78

3.3 Accuracy of AD/CN classification

Results of experiments of AD/CN classification on ADNI and OASIS datasets are listed in Table 2. Similarly, two baselines are tested and their accuracy and F1 score are increased by 6 and 7 points on average, respectively. Noteworthy, GCN is unstable on the ADNI dataset since the standard deviation on accuracy

and F1 score is over 30. In comparison, SFDN on 5-fold cross-validation is more stable and shows an improvement from 54.07 to 74.07 of average accuracy.

4 Conclusion

In summary, this paper introduces detour connectivity (DC) as a novel measurement to explore the relationship between structural connectivity (SC) and functional connectivity (FC) in neuroscience field. DC considers indirect anatomical routes, weighting functional connection strength. Additionally, we propose the SC-FC Detour Network (SFDN), a Transformer-style graph neural network that integrates DC embedding into node features through a self-attention mechanism. Evaluations of the proposed methods on three public datasets reveal the effectiveness of SFDN in cognitive state and disease classifications. Results of t-tests for DC between groups of the cognitive state provide interpretable evidence by the distinct detection of macroscale brain network community to support the improvement of SFDN.
Discussions. The limitation of our approach is a lack of consideration about directed SC, negative FC, and connections between hemispheres.

Disclosure of Interests . The authors have no competing interests to declare.

References

1. Antonopoulos, N., Veglis, A., Gardikiotis, A., Kotsakis, R., Kalliris, G.: Web third-person effect in structural aspects of the information on media websites. Computers in human behavior **44**, 48–58 (2015)
2. Baum, G.L., Cui, Z., Roalf, D.R., Ciric, R., Betzel, R.F., Larsen, B., Cieslak, M., Cook, P.A., Xia, C.H., Moore, T.M., et al.: Development of structure–function coupling in human brain networks during youth. Proceedings of the National Academy of Sciences **117**(1), 771–778 (2020)
3. Betzel, R.F., Medaglia, J.D., Bassett, D.S.: Diversity of meso-scale architecture in human and non-human connectomes. Nature communications **9**(1), 346 (2018)
4. Bookheimer, S.Y., Salat, D.H., Terpstra, M., Ances, B.M., Barch, D.M., Buckner, R.L., Burgess, G.C., Curtiss, S.W., Diaz-Santos, M., Elam, J.S., et al.: The lifespan human connectome project in aging: an overview. Neuroimage **185**, 335–348 (2019)
5. Calhoun, V.D., Amin, M.F., Hjelm, D., Damaraju, E., Plis, S.M.: A deep-learning approach to translate between brain structure and functional connectivity. In: 2017 IEEE International Conference on Acoustics, Speech and Signal Processing (ICASSP). pp. 6155–6159. IEEE (2017)
6. Chartrand, G., Johns, G.L., Tian, S.: Detour distance in graphs. In: Annals of discrete mathematics, vol. 55, pp. 127–136. Elsevier (1993)
7. Damoiseaux, J.S., Greicius, M.D.: Greater than the sum of its parts: a review of studies combining structural connectivity and resting-state functional connectivity. Brain structure and function **213**, 525–533 (2009)
8. Destrieux, C., Fischl, B., Dale, A., Halgren, E.: Automatic parcellation of human cortical gyri and sulci using standard anatomical nomenclature. Neuroimage **53**(1), 1–15 (2010)

9. Feng, X., Sun, H., Wu, J., Lv, Y., Zhi, D.: Understanding detour behavior in taxi services: A combined approach. Transportation Research Part C: Emerging Technologies **145**, 103950 (2022)
10. Goñi, J., Van Den Heuvel, M.P., Avena-Koenigsberger, A., Velez de Mendizabal, N., Betzel, R.F., Griffa, A., Hagmann, P., Corominas-Murtra, B., Thiran, J.P., Sporns, O.: Resting-brain functional connectivity predicted by analytic measures of network communication. Proceedings of the National Academy of Sciences **111**(2), 833–838 (2014)
11. Gordon, E.M., Laumann, T.O., Adeyemo, B., Huckins, J.F., Kelley, W.M., Petersen, S.E.: Generation and evaluation of a cortical area parcellation from resting-state correlations. Cerebral cortex **26**(1), 288–303 (2016)
12. Hirota, M., Oda, T., Endo, M., Ishikawa, H.: Generating distributed representation of user movement for extracting detour spots. In: Proceedings of the 11th International Conference on Management of Digital EcoSystems. pp. 250–255 (2019)
13. Honey, C.J., Sporns, O., Cammoun, L., Gigandet, X., Thiran, J.P., Meuli, R., Hagmann, P.: Predicting human resting-state functional connectivity from structural connectivity. Proceedings of the National Academy of Sciences **106**(6), 2035–2040 (2009)
14. Honey, C.J., Thivierge, J.P., Sporns, O.: Can structure predict function in the human brain? Neuroimage **52**(3), 766–776 (2010)
15. Kipf, T.N., Welling, M.: Semi-supervised classification with graph convolutional networks. arXiv preprint arXiv:1609.02907 (2016)
16. LaMontagne, P.J., Benzinger, T.L., Morris, J.C., Keefe, S., Hornbeck, R., Xiong, C., Grant, E., Hassenstab, J., Moulder, K., Vlassenko, A.G., et al.: Oasis-3: longitudinal neuroimaging, clinical, and cognitive dataset for normal aging and alzheimer disease. MedRxiv pp. 2019–12 (2019)
17. Liu, H., Dan, T., Huang, Z., Yang, D., Kim, W.H., Kim, M., Laurienti, P., Wu, G.: Holobrain: A harmonic holography for self-organized brain function. In: International Conference on Information Processing in Medical Imaging. pp. 29–40. Springer (2023)
18. Liu, Z.Q., Betzel, R.F., Misic, B.: Benchmarking functional connectivity by the structure and geometry of the human brain. Network Neuroscience **6**(4), 937–949 (2022)
19. Luo, Y., Kong, F., Qi, S., You, X., Huang, X.: Resting-state functional connectivity of the default mode network associated with happiness. Social cognitive and affective neuroscience **11**(3), 516–524 (2016)
20. Mišić, B., Betzel, R.F., De Reus, M.A., Van Den Heuvel, M.P., Berman, M.G., McIntosh, A.R., Sporns, O.: Network-level structure-function relationships in human neocortex. Cerebral Cortex **26**(7), 3285–3296 (2016)
21. Mišić, B., Betzel, R.F., Nematzadeh, A., Goni, J., Griffa, A., Hagmann, P., Flammini, A., Ahn, Y.Y., Sporns, O.: Cooperative and competitive spreading dynamics on the human connectome. Neuron **86**(6), 1518–1529 (2015)
22. Neudorf, J., Kress, S., Borowsky, R.: Structure can predict function in the human brain: a graph neural network deep learning model of functional connectivity and centrality based on structural connectivity. Brain Structure and Function pp. 1–13 (2022)
23. Park, H.J., Friston, K.: Structural and functional brain networks: From connections to cognition. Science **342**(6158), 1238411 (2013)
24. Preti, M.G., Van De Ville, D.: Decoupling of brain function from structure reveals regional behavioral specialization in humans. Nature communications **10**(1), 4747 (2019)

25. Sarwar, T., Tian, Y., Yeo, B.T., Ramamohanarao, K., Zalesky, A.: Structure-function coupling in the human connectome: A machine learning approach. NeuroImage **226**, 117609 (2021)
26. Tzourio-Mazoyer, N., Landeau, B., Papathanassiou, D., Crivello, F., Etard, O., Delcroix, N., Mazoyer, B., Joliot, M.: Automated anatomical labeling of activations in spm using a macroscopic anatomical parcellation of the mni mri single-subject brain. Neuroimage **15**(1), 273–289 (2002)
27. Wang, P., Kong, R., Kong, X., Liégeois, R., Orban, C., Deco, G., Van Den Heuvel, M.P., Thomas Yeo, B.: Inversion of a large-scale circuit model reveals a cortical hierarchy in the dynamic resting human brain. Science advances **5**(1), eaat7854 (2019)
28. Weiner, M.W., Veitch, D.P., Aisen, P.S., Beckett, L.A., Cairns, N.J., Cedarbaum, J., Donohue, M.C., Green, R.C., Harvey, D., Jack Jr, C.R., et al.: Impact of the alzheimer's disease neuroimaging initiative, 2004 to 2014. Alzheimer's & Dementia **11**(7), 865–884 (2015)
29. Xu, K., Hu, W., Leskovec, J., Jegelka, S.: How powerful are graph neural networks? arXiv preprint arXiv:1810.00826 (2018)
30. Zamani Esfahlani, F., Faskowitz, J., Slack, J., Mišić, B., Betzel, R.F.: Local structure-function relationships in human brain networks across the lifespan. Nature communications **13**(1), 2053 (2022)